An aerial satellite image of a cropland area, overlaid with a semi-transparent grid and various colored polygons (green, brown, red, yellow) representing different crop types or classifications. The text is centered on the image.

Automatic and Extensive Cropland Classification Based on Satellite Data

Andrés Farall
Ecoclimasol

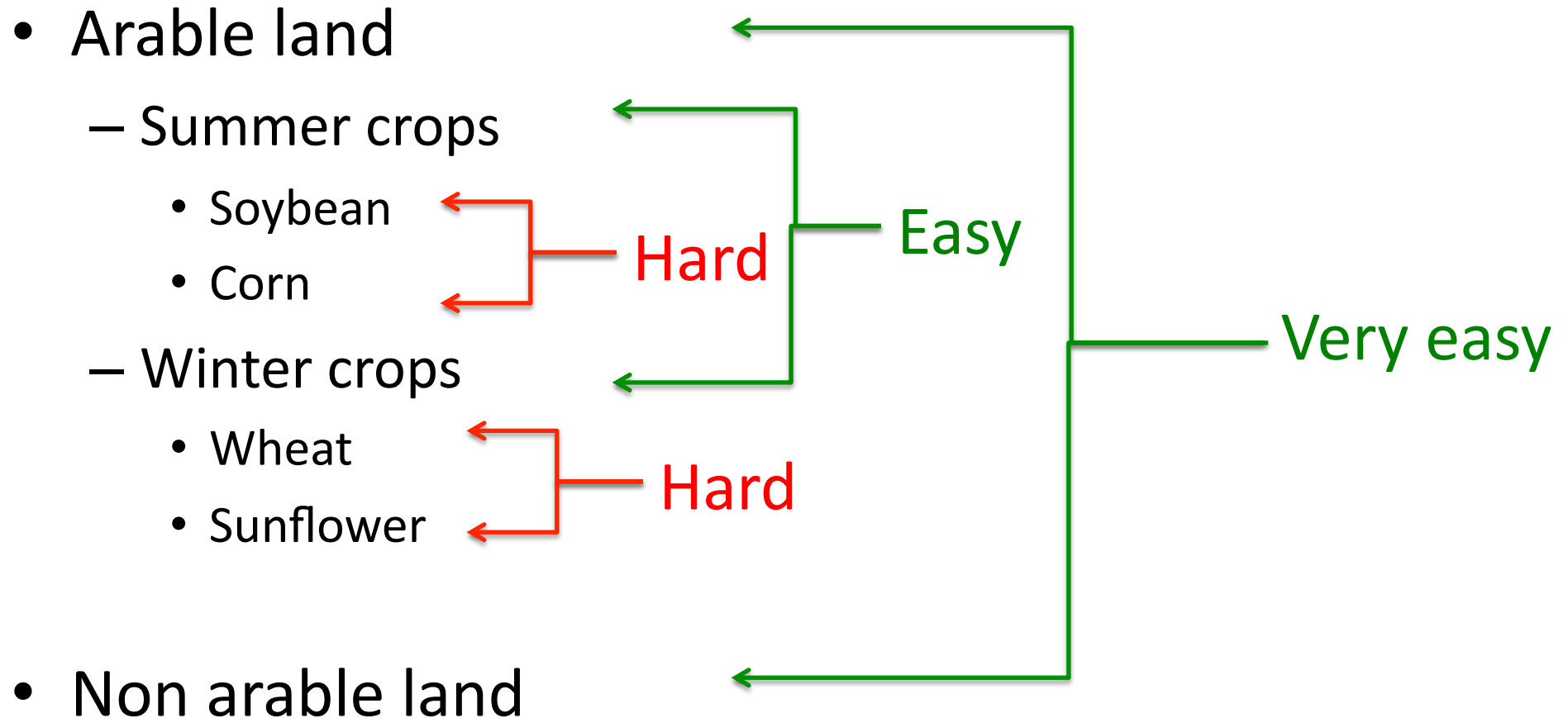
Why Automatic Crop Classification ?

- Crops in **Argentina**: ~ 34.000.000 has, ~ 400.000 fields
- Screening of **unknown regions**
- Global yield estimation and **tax evasion** control
- Valuable **information** for agro-related and agro-insurance companies
- Precise **georeference** of croplands
- Global crop **area assesment** and **yield estimation**

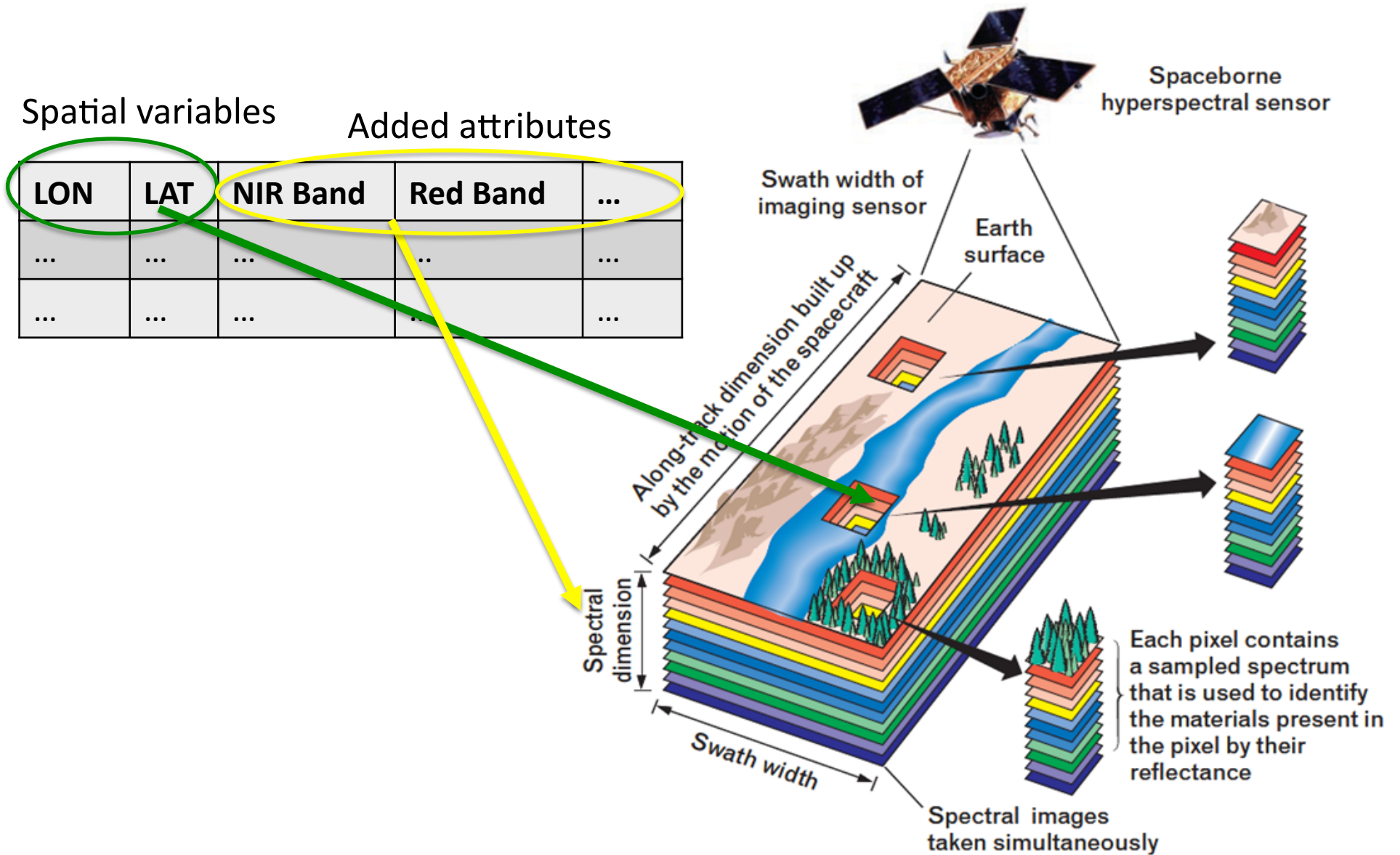
Some Specific Classification Goals

- To assess **crop share** (relative proportions) in a large area (no georeference available of the fields)
- To estimate **yield of an specific crop/season** in a large area (no georeference available of the fields)
- To detect and **to georeference fields** with specific crops (no georeference available of the fields)
- To detect **kind-of-crop info** from specific fields (available georeference of the fields)

Kind of Crops to be Detected



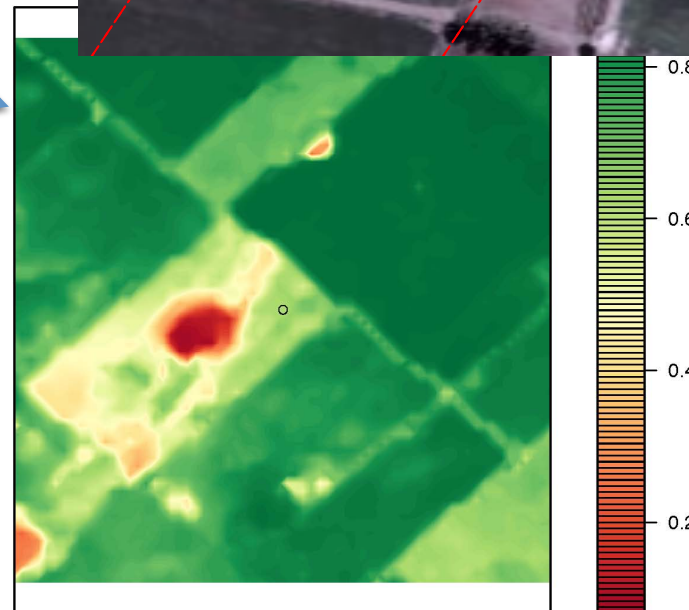
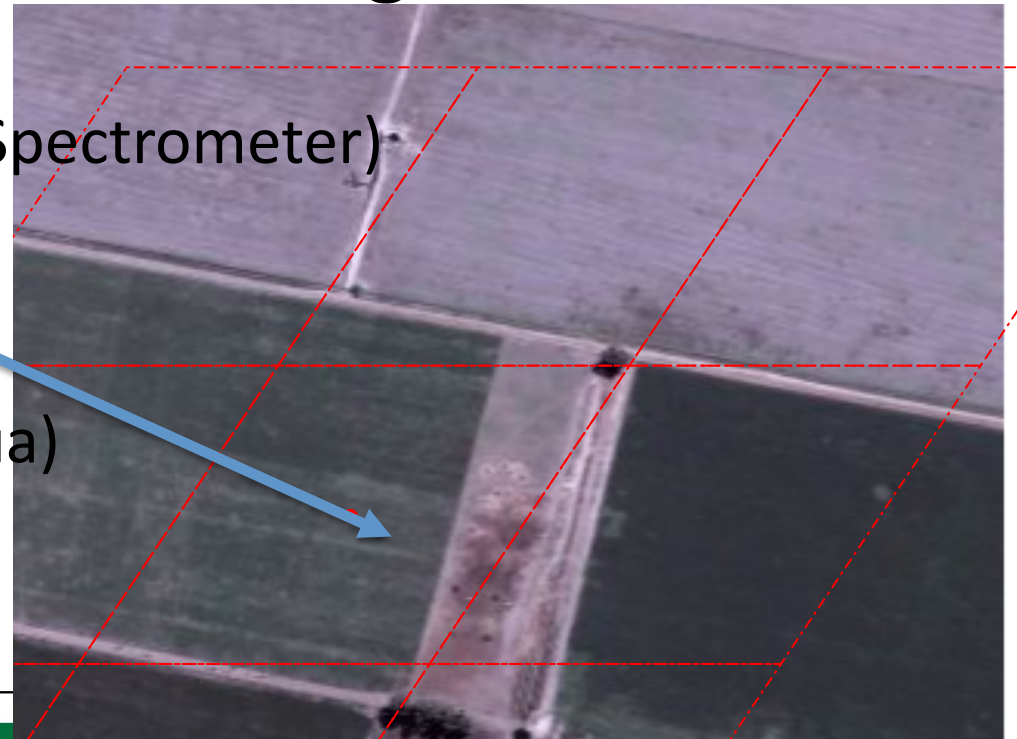
Remote Sensing Instruments



source : <http://www.markelowitz.com/Hyperspectral.html>

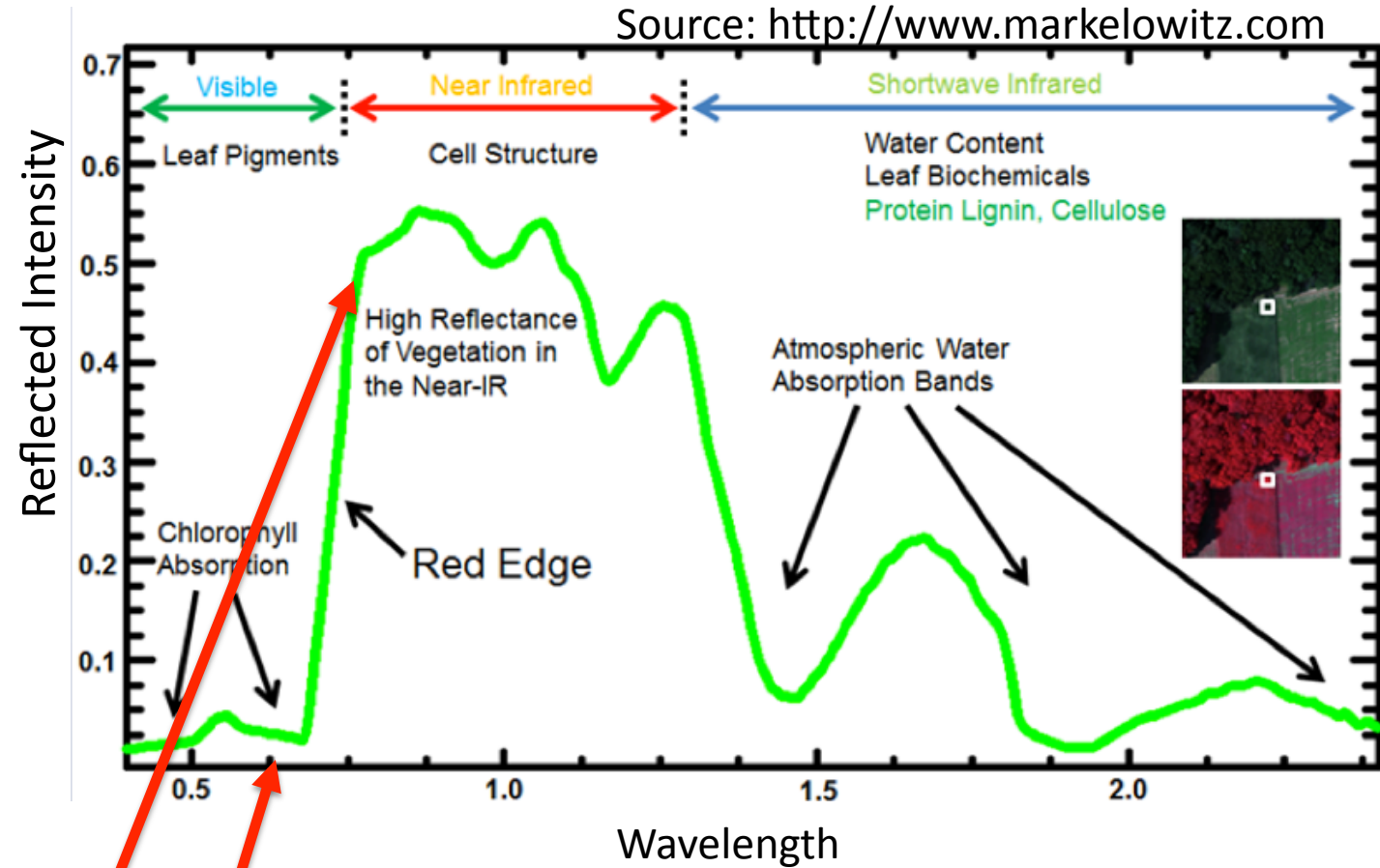
Main Available Remote Sensing Instruments

- MODIS (MODerate Imaging Spectrometer)
 - 250m X 250m
 - 2 images per day
 - 2 satellites (Terra and Aqua)
 - 36 spectral bands
- LANDSAT 8
 - 15m X 15m (interpolated)
 - 1 image every 16 days
 - 1 satellite
 - 11 bands



Vegetation Indices (VIs)

- CI
- EVI
- ENVI
- **NDVI**

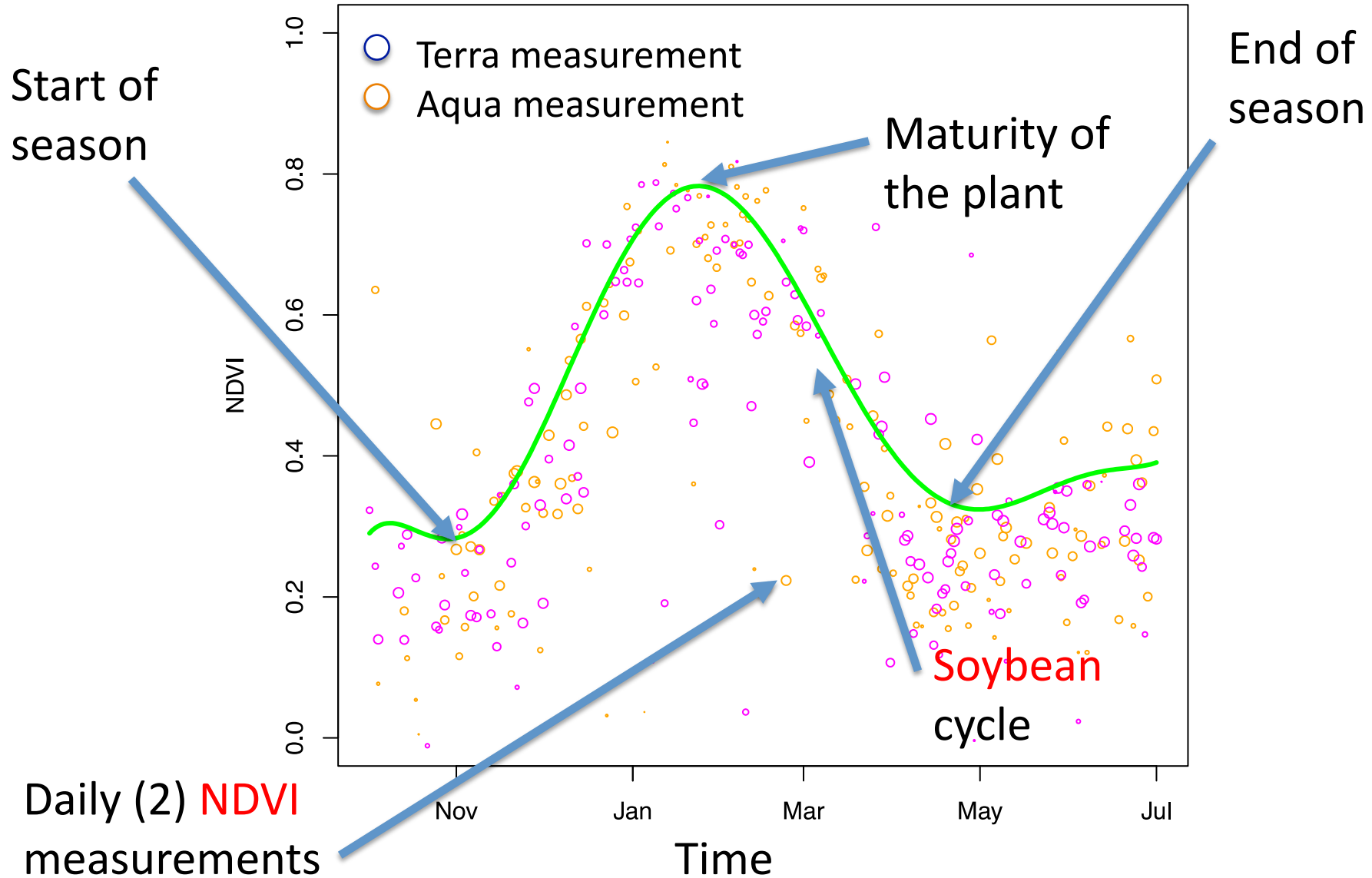


$$\text{NDVI} = \frac{\text{NIR} - \text{Red}}{\text{NIR} + \text{Red}}$$

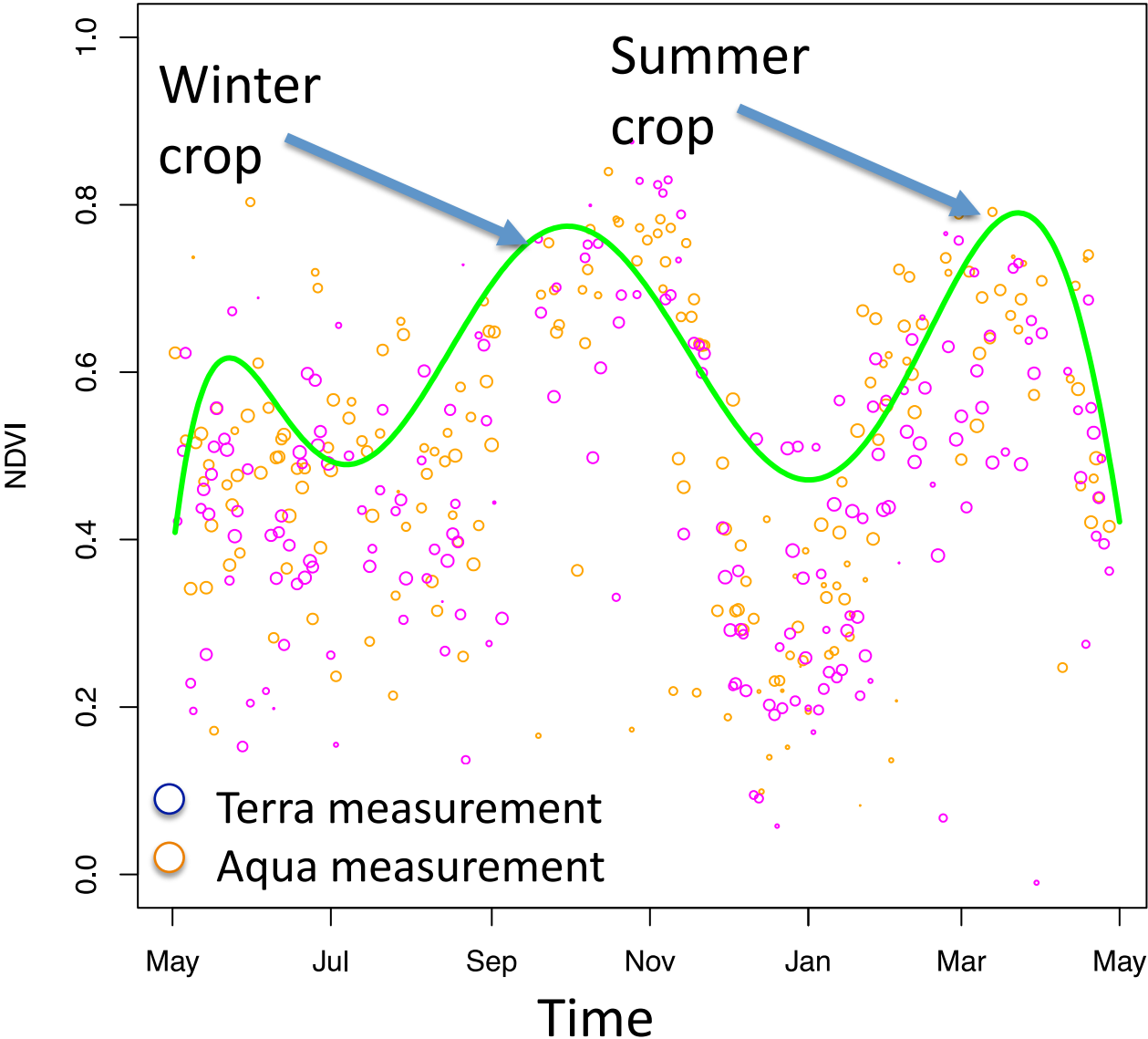
In general
 $-1 \leq \text{NDVI} \leq 1$

For plants
 $0 \leq \text{NDVI} \leq 1$

How is a Typical Phenological Crop Cycle ?

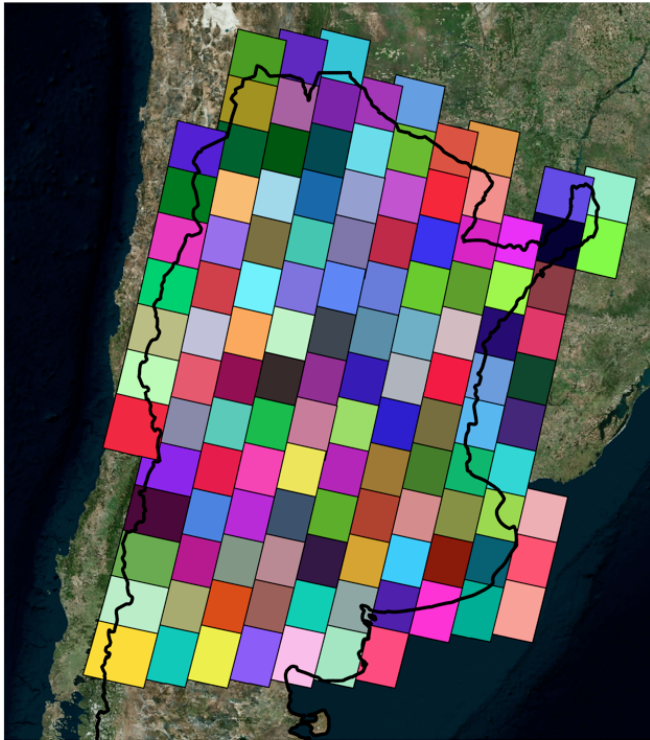


Double-Crop Phenological Cycle

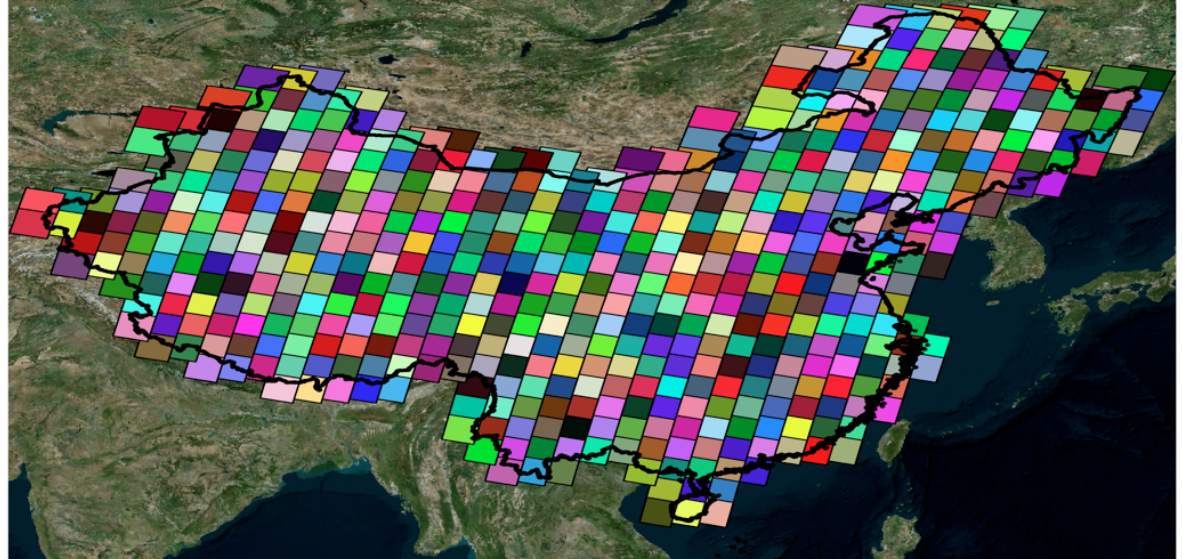


Landsat: Big Data !

Argentina



China



Landsat tile = 185km X 185 km

~ 17.500px X 14.500 px

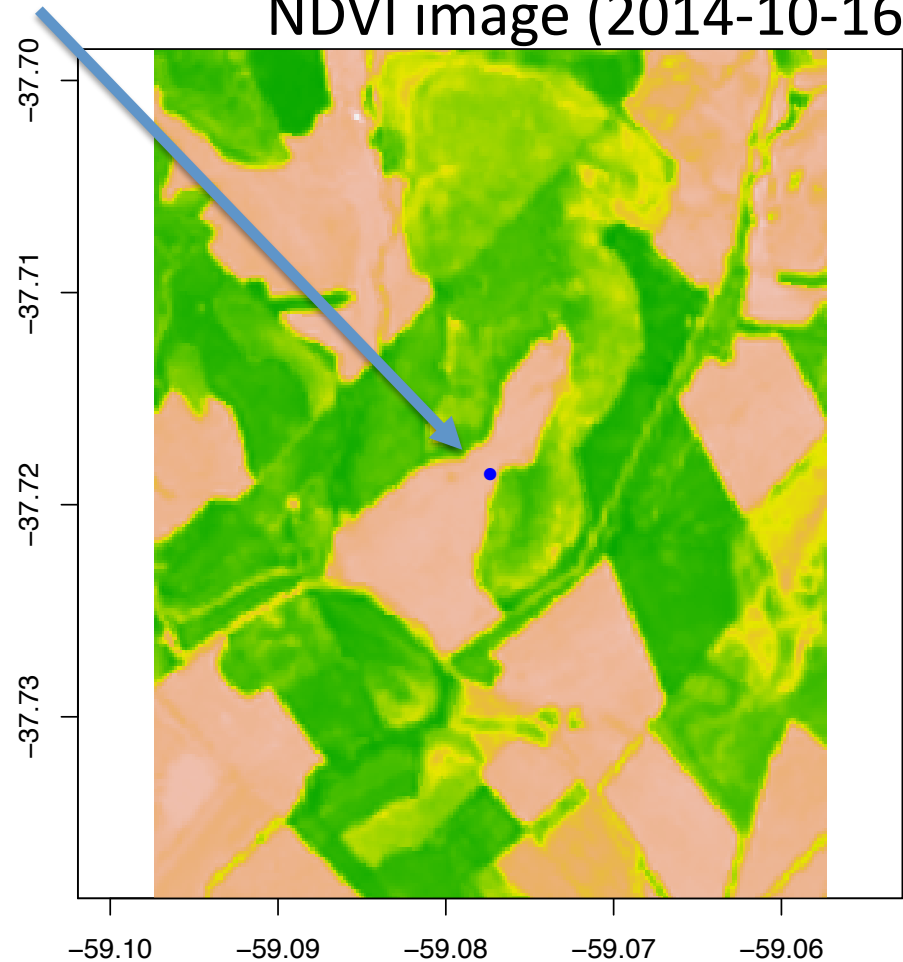
	Size of 1 tile	Number of tiles	Frequency	Size
Argentina	950 Mb	123	23 per year	2,6 Tb
China	950 Mb	530	23 per year	11,1 Tb

Cropland Detection Using Landsat 8 Unsupervised Approach

Visible image from
Open Street Map

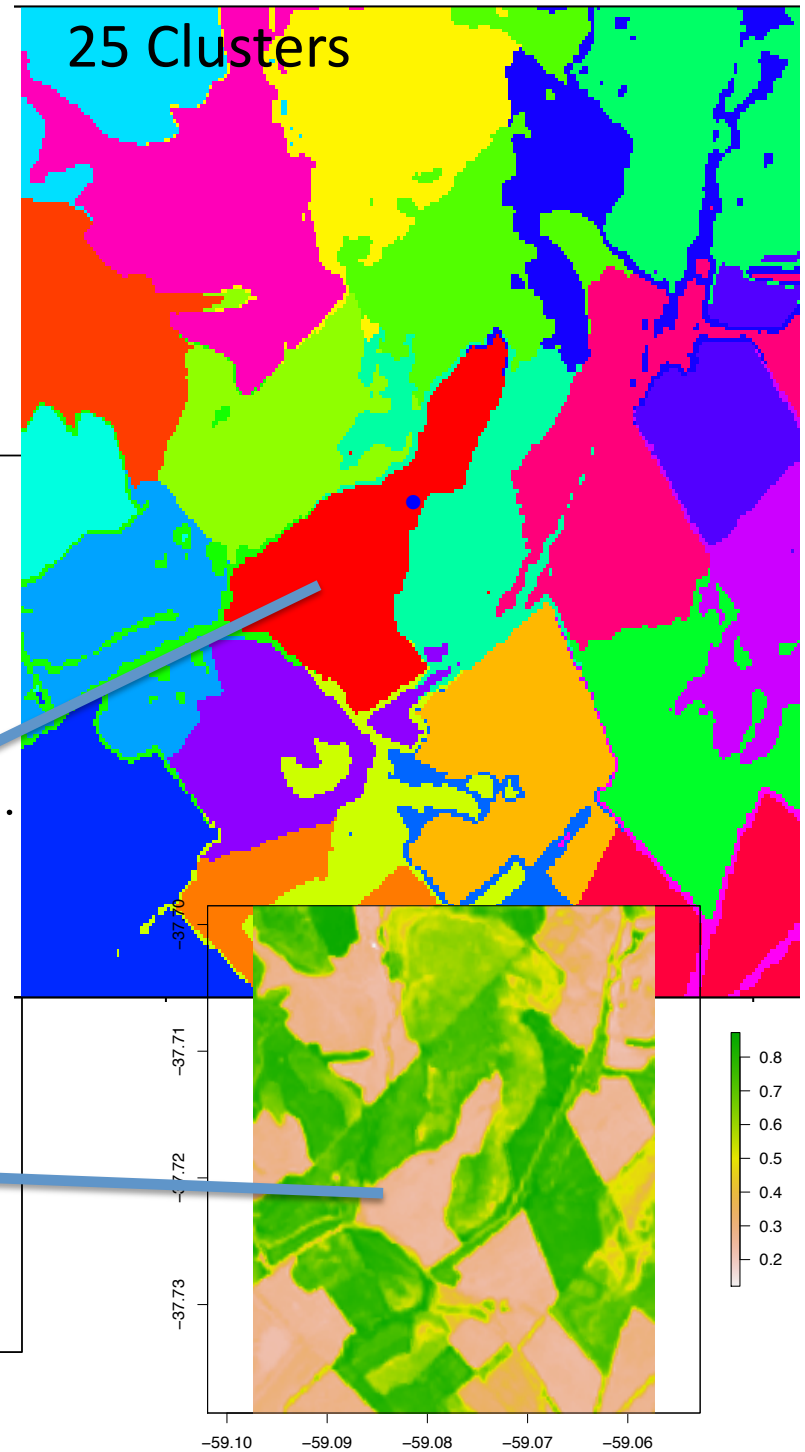
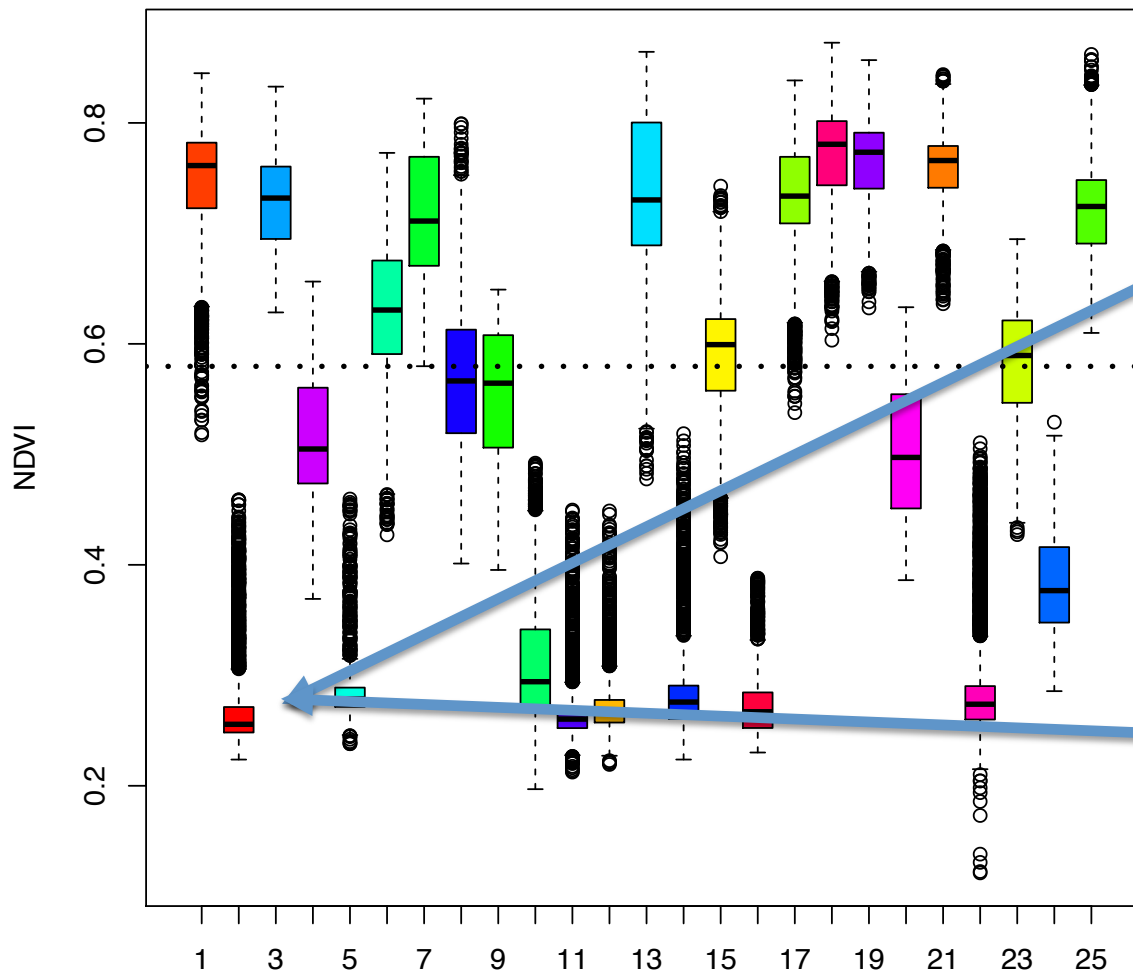


Point of
interest



Single Image Clustering based on $X + Y + \text{NDVI}$

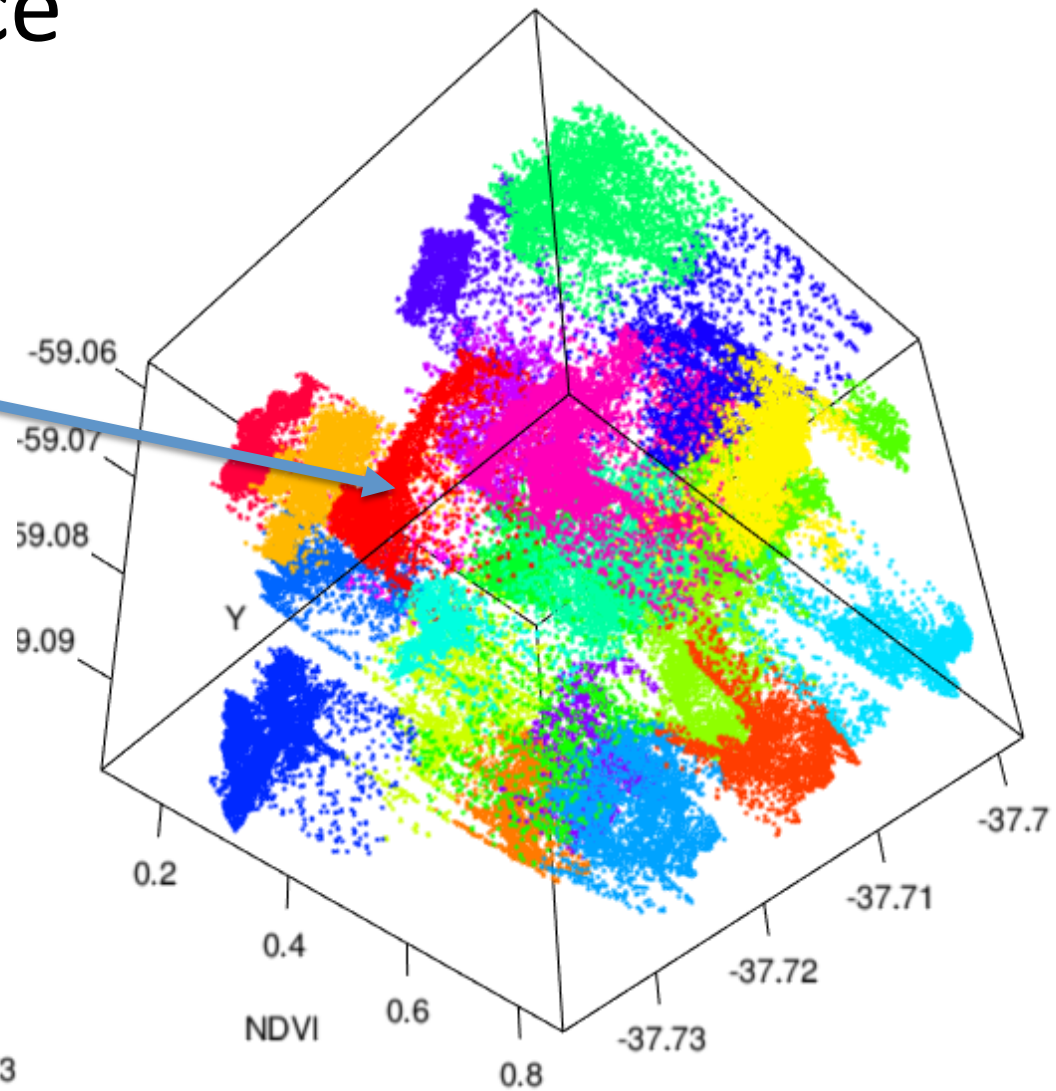
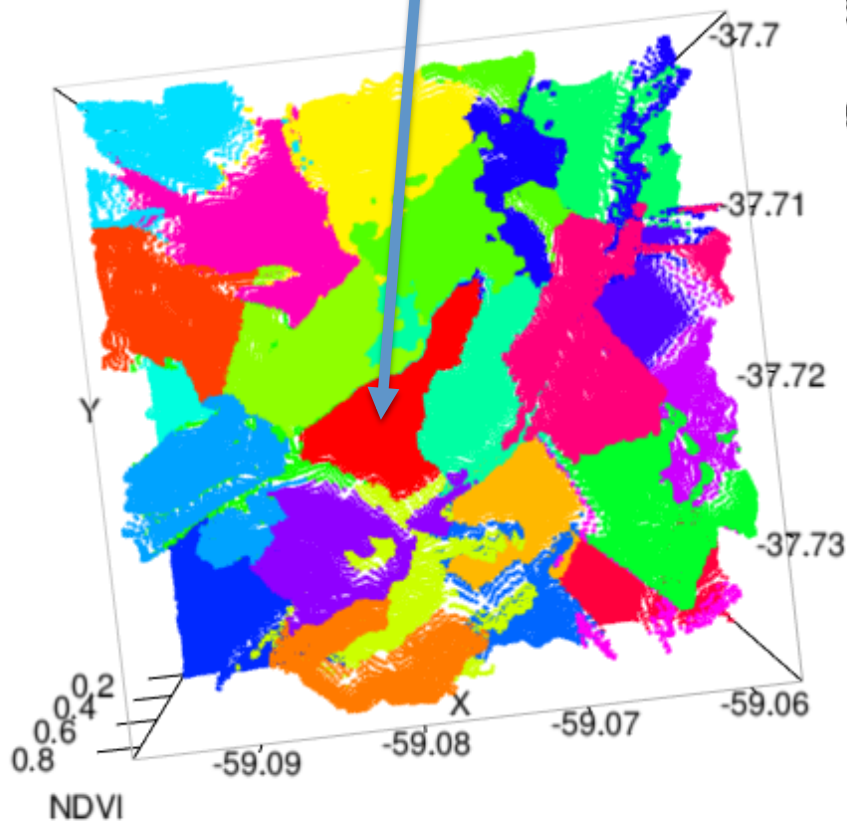
Feature
space



The Feature Space

$X + Y + \text{NDVI}$

Field of interest

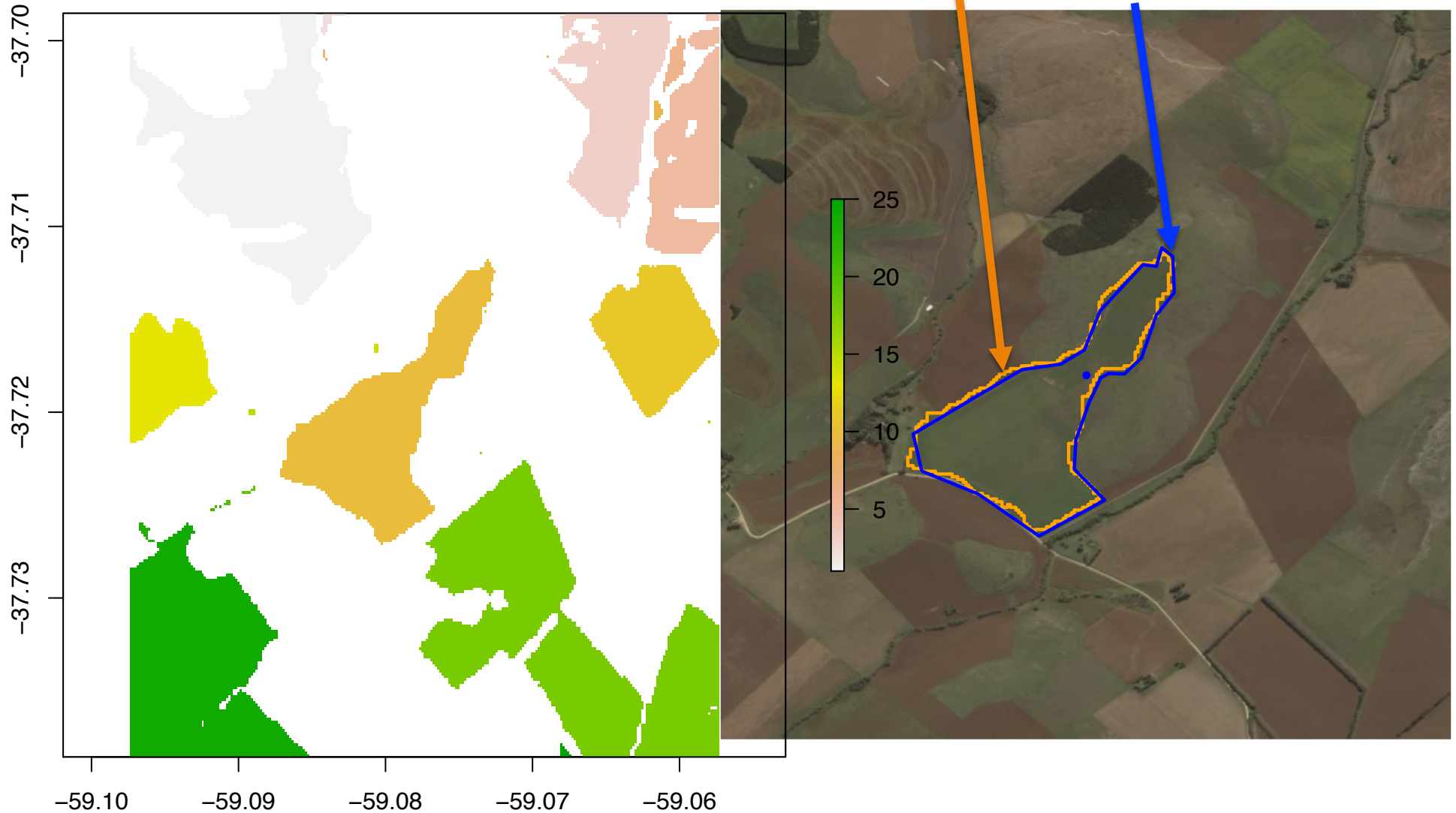


Field Detected

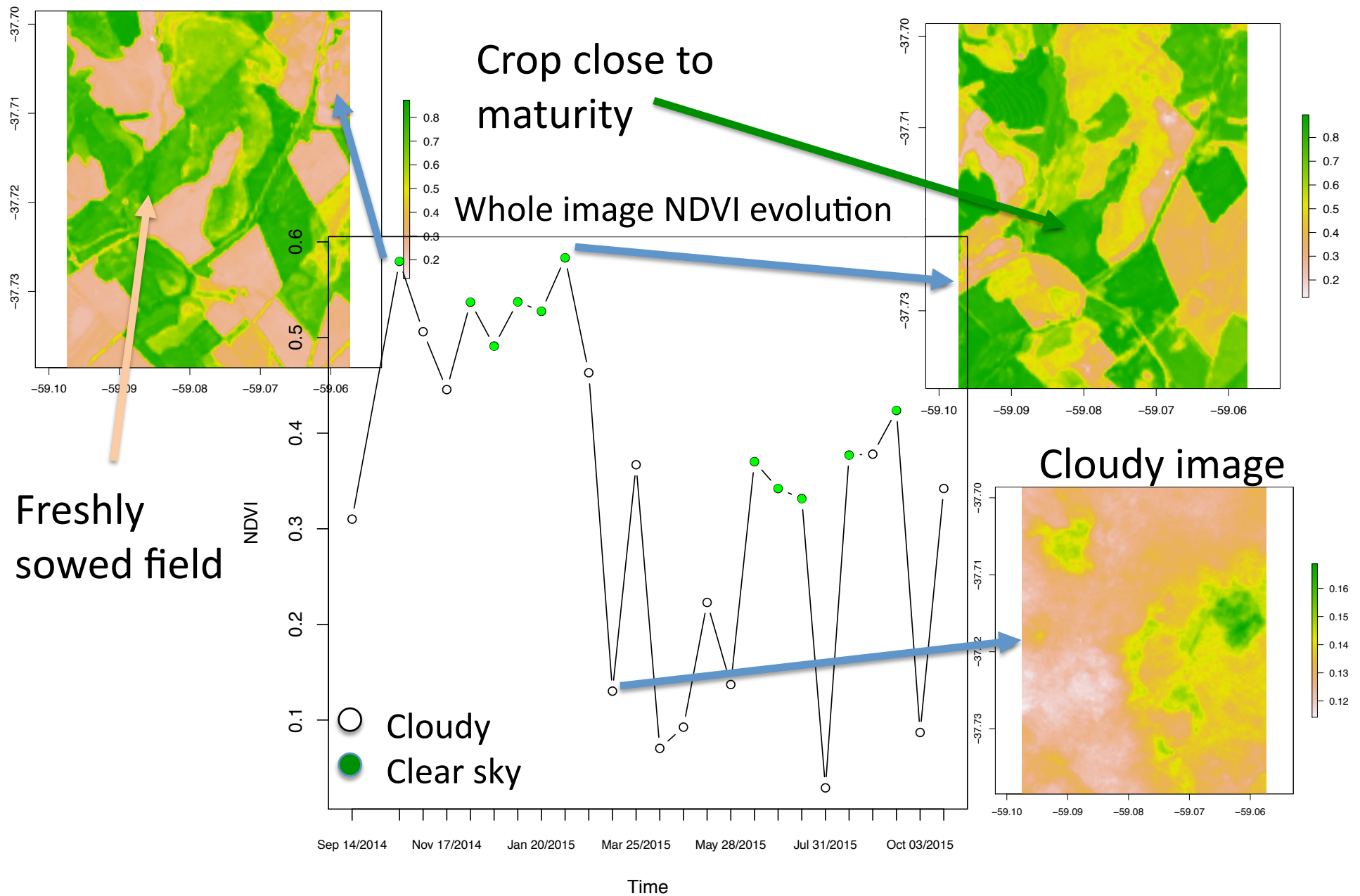
Actual
georeferenced
field

Polygon induced
by the method

Clusters of similar NDVI values



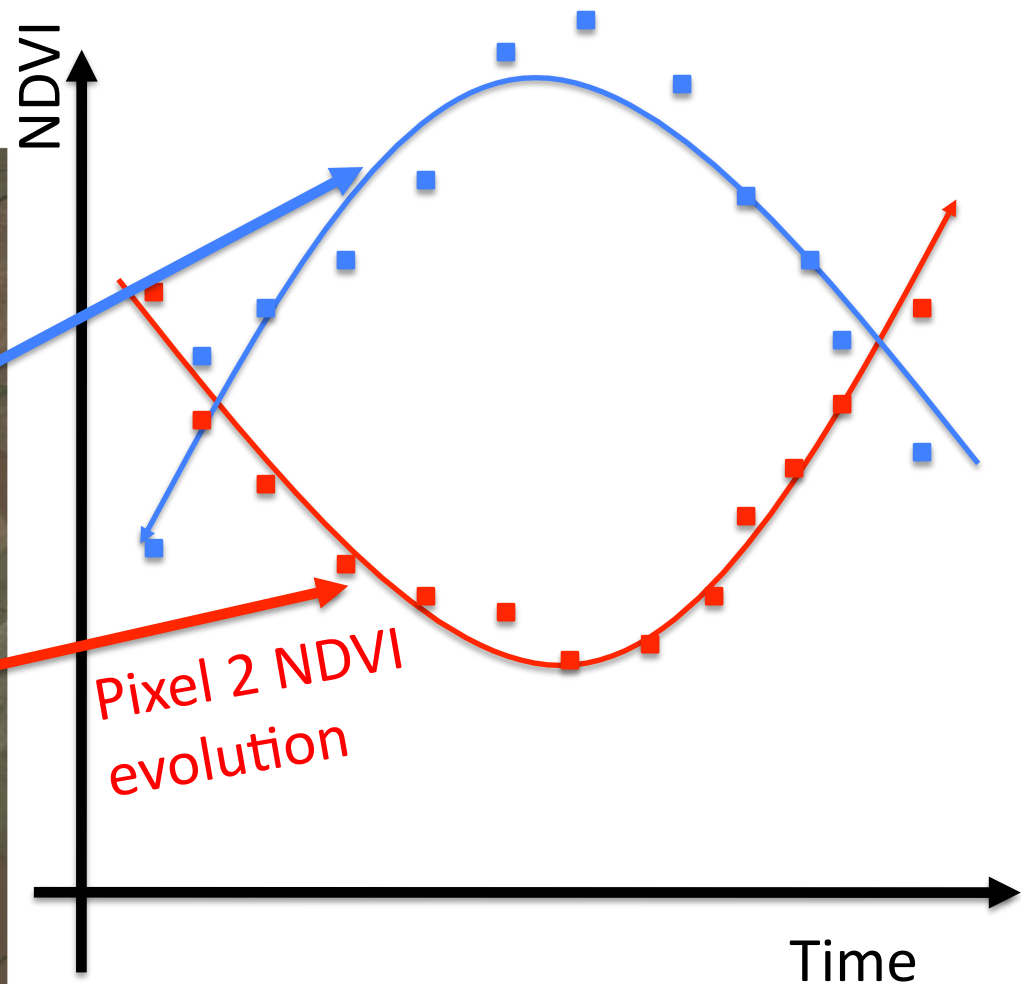
Time series of Landsat images



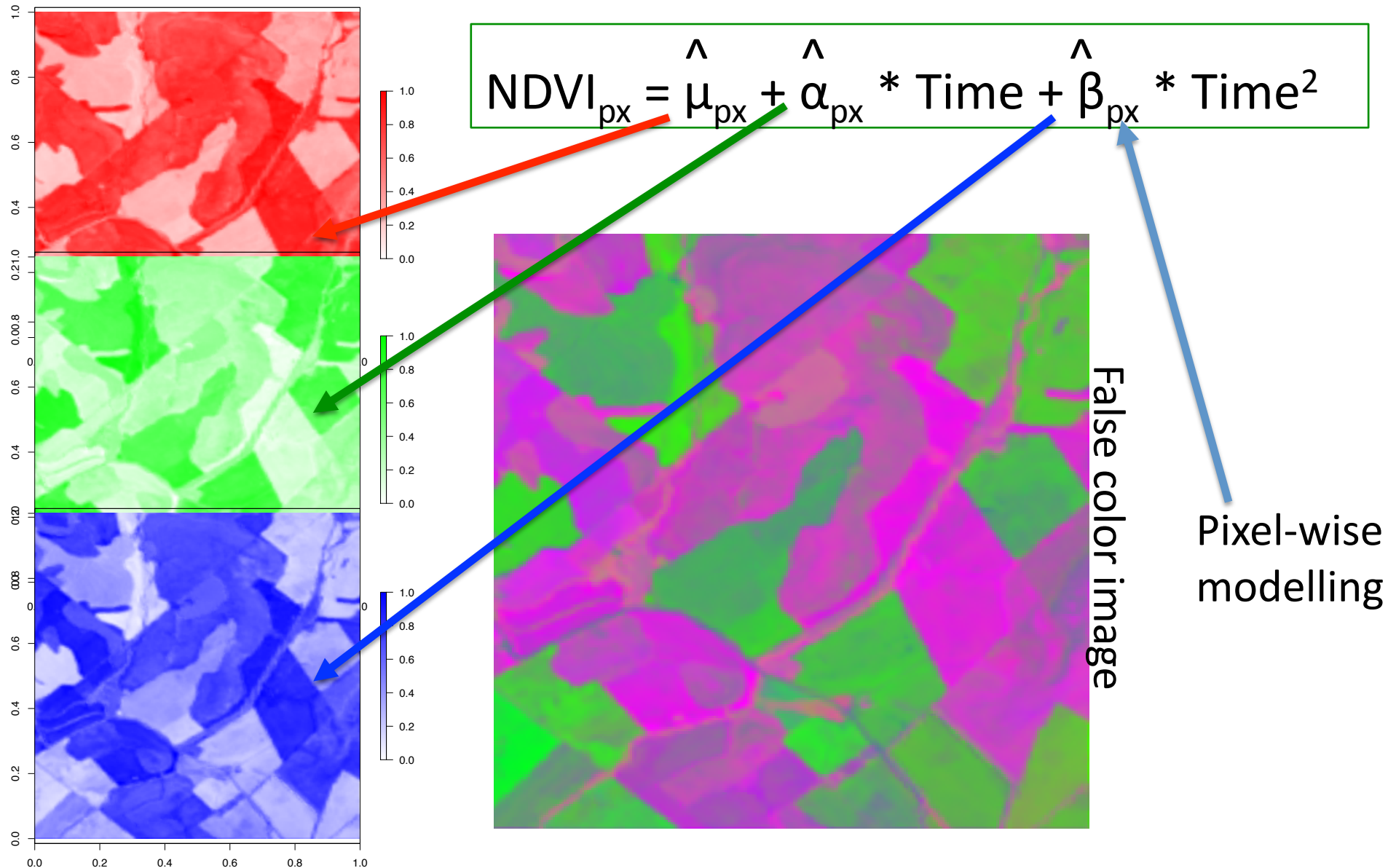
Working With a Temporal Ensemble of Images

$$\text{NDVI}_{\text{px}} = \mu_{\text{px}} + \alpha_{\text{px}} * \text{Time} + \beta_{\text{px}} * \text{Time}^2$$

Pixel-wise
modelling



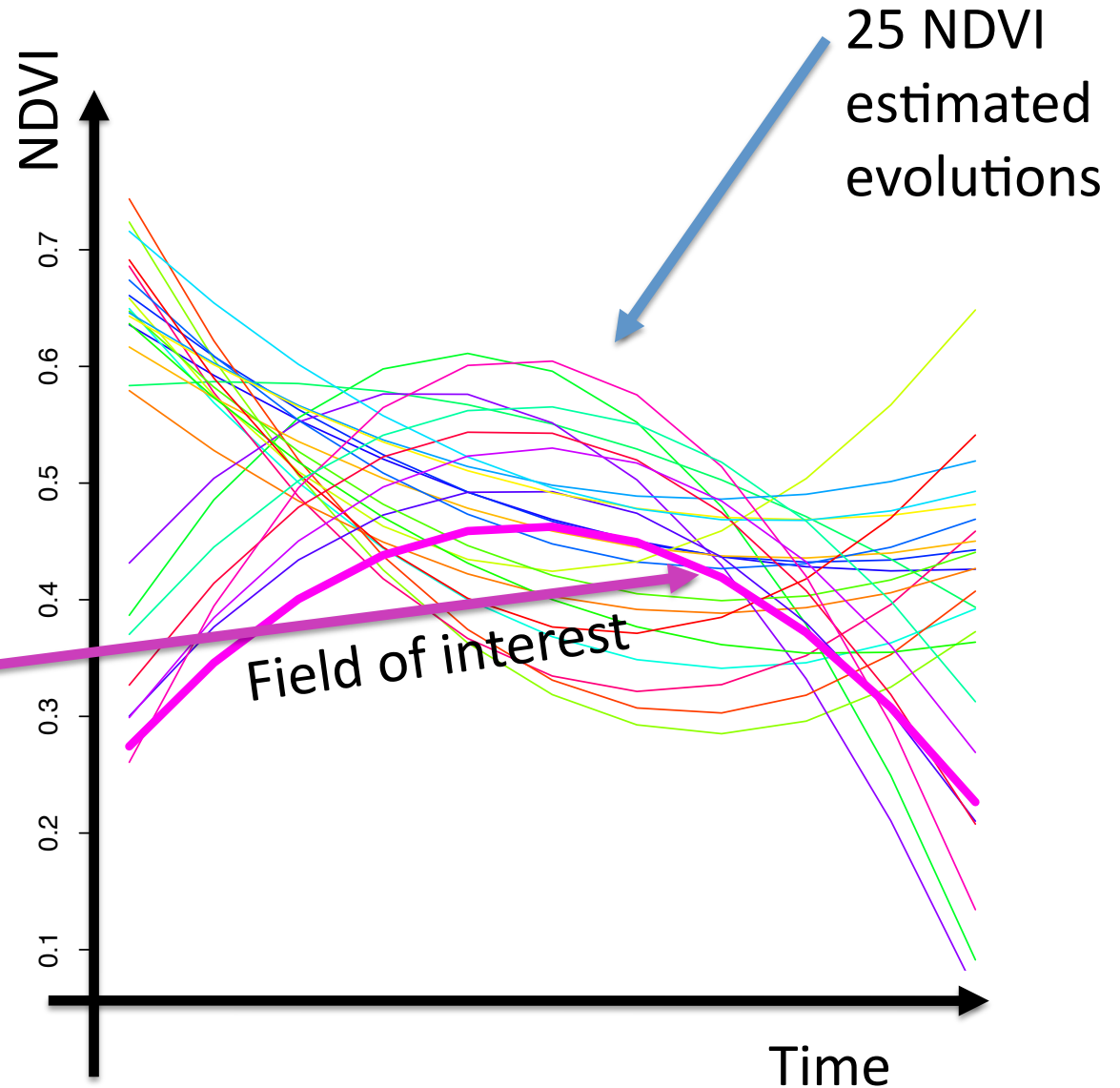
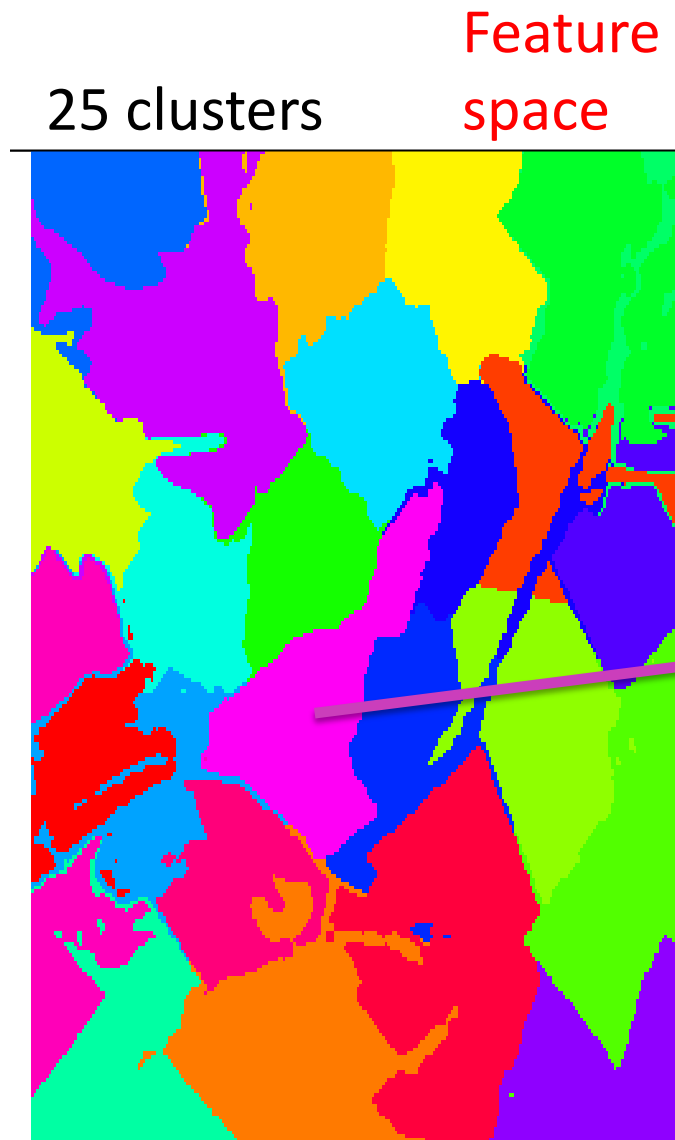
Added Attributes Based on Statistical Modelling of NDVI Temporal Evolution



Clustering Based on Modelled NDVI

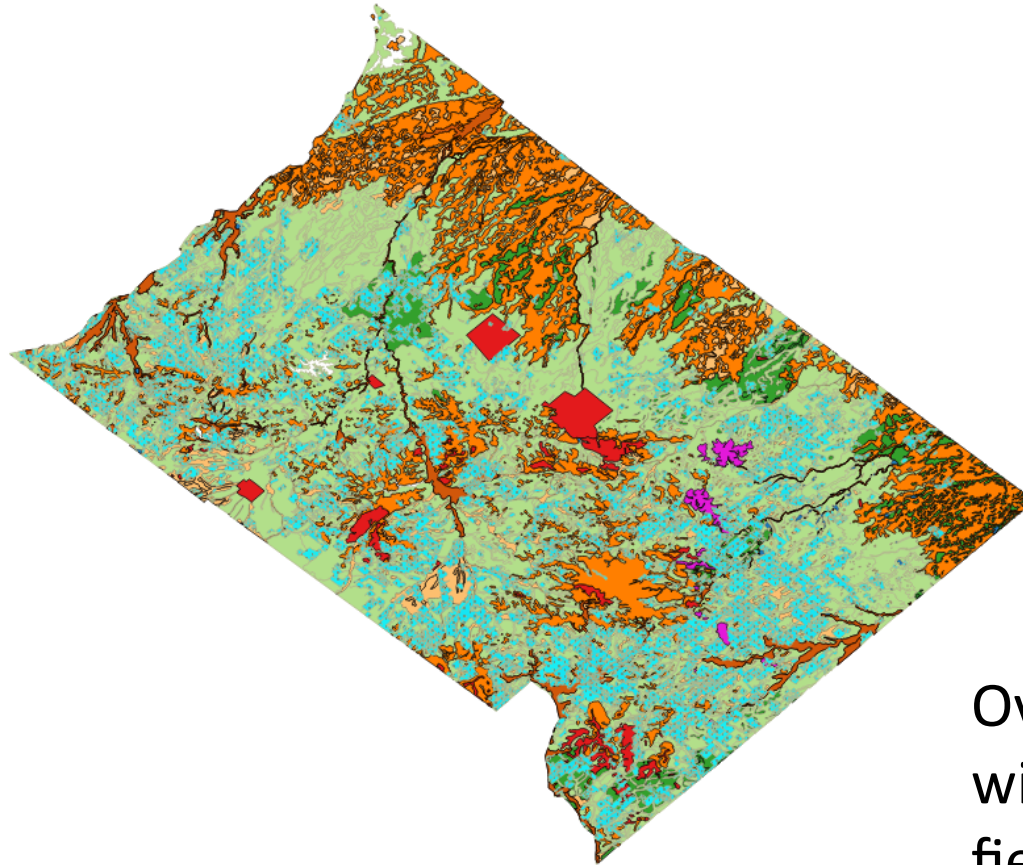
$$X + Y + \mu + \alpha + \beta$$

Temporal Evolution



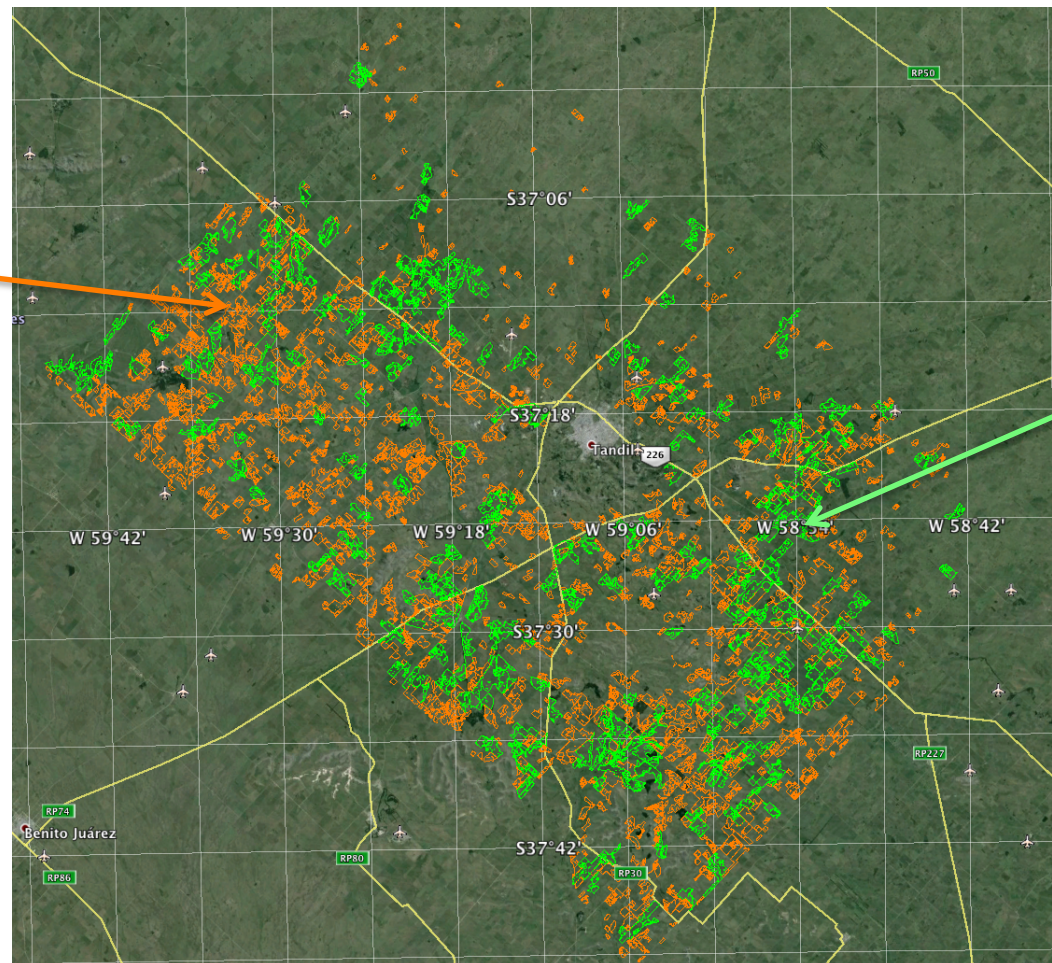
Agreement Between Detected Fields and Soil Capability (Tandil)

Soil
management
capability



Overlapping
with sowed
fields
automatically
detected

Automatic Detection of Summer and Winter Crops in Tandil



Winter crop

Estimation:
89.000 has

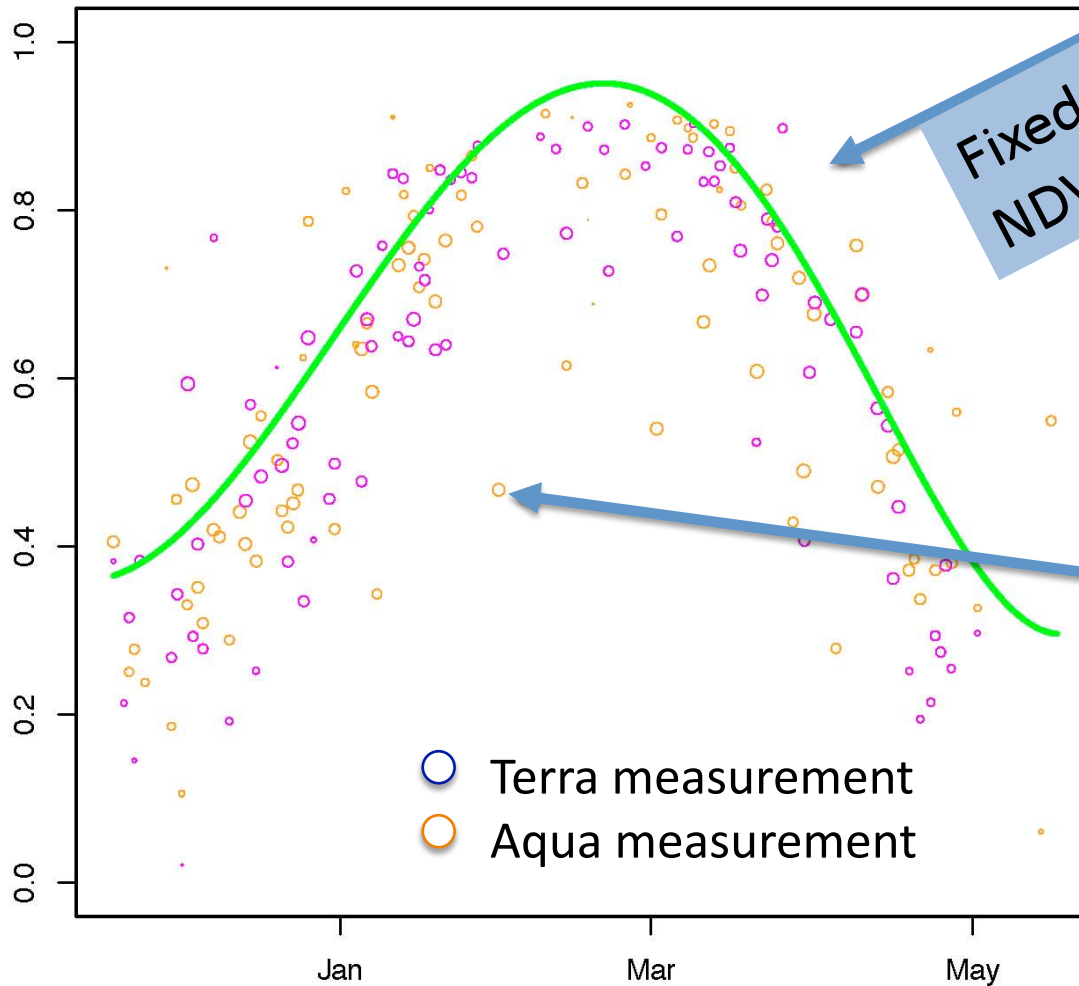
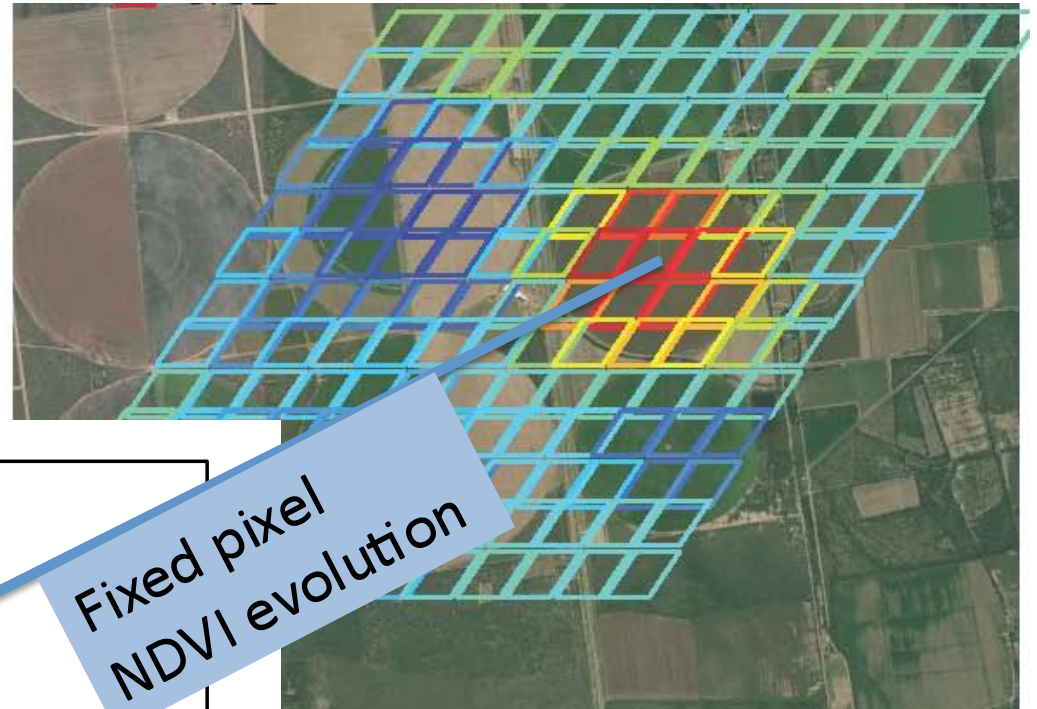
MAGyP (2014):
85.000 has

Summer crop

Estimation:
200.000has

MAGyP (2013) :
216.000 has

Cropland Detection Using MODIS (Supervised Approach)



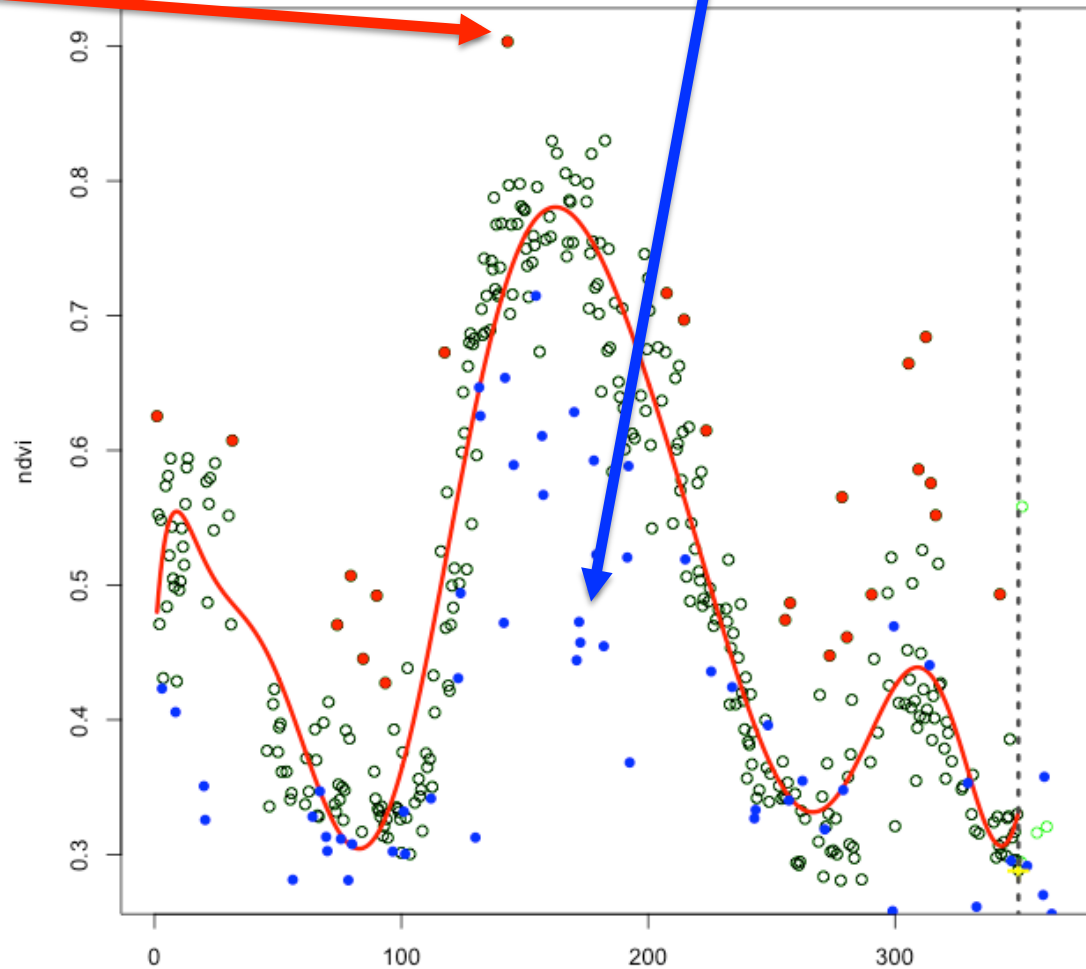
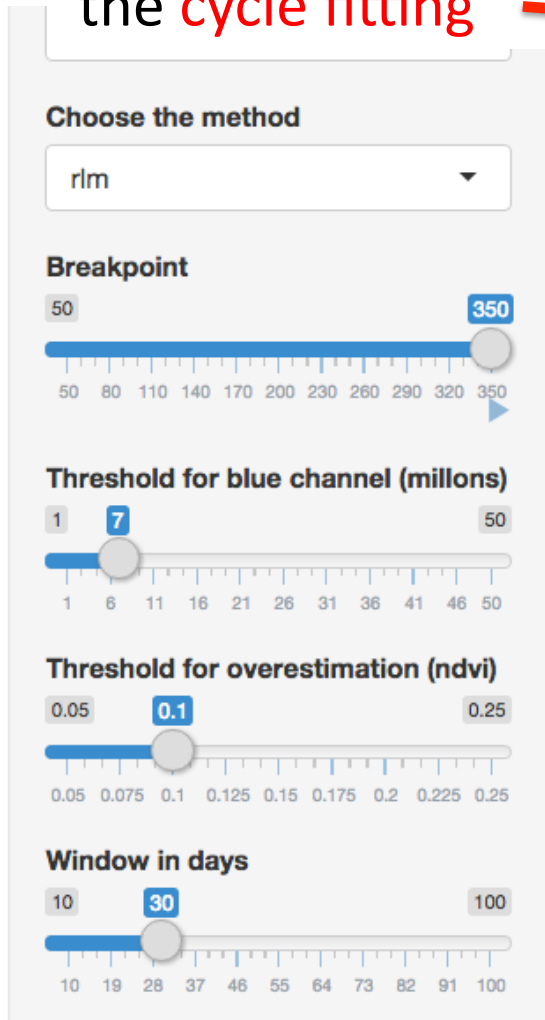
Fixed pixel
NDVI evolution

Dot size
proportional to the
reliability of the
measurement

Fitting the Crop Cycle

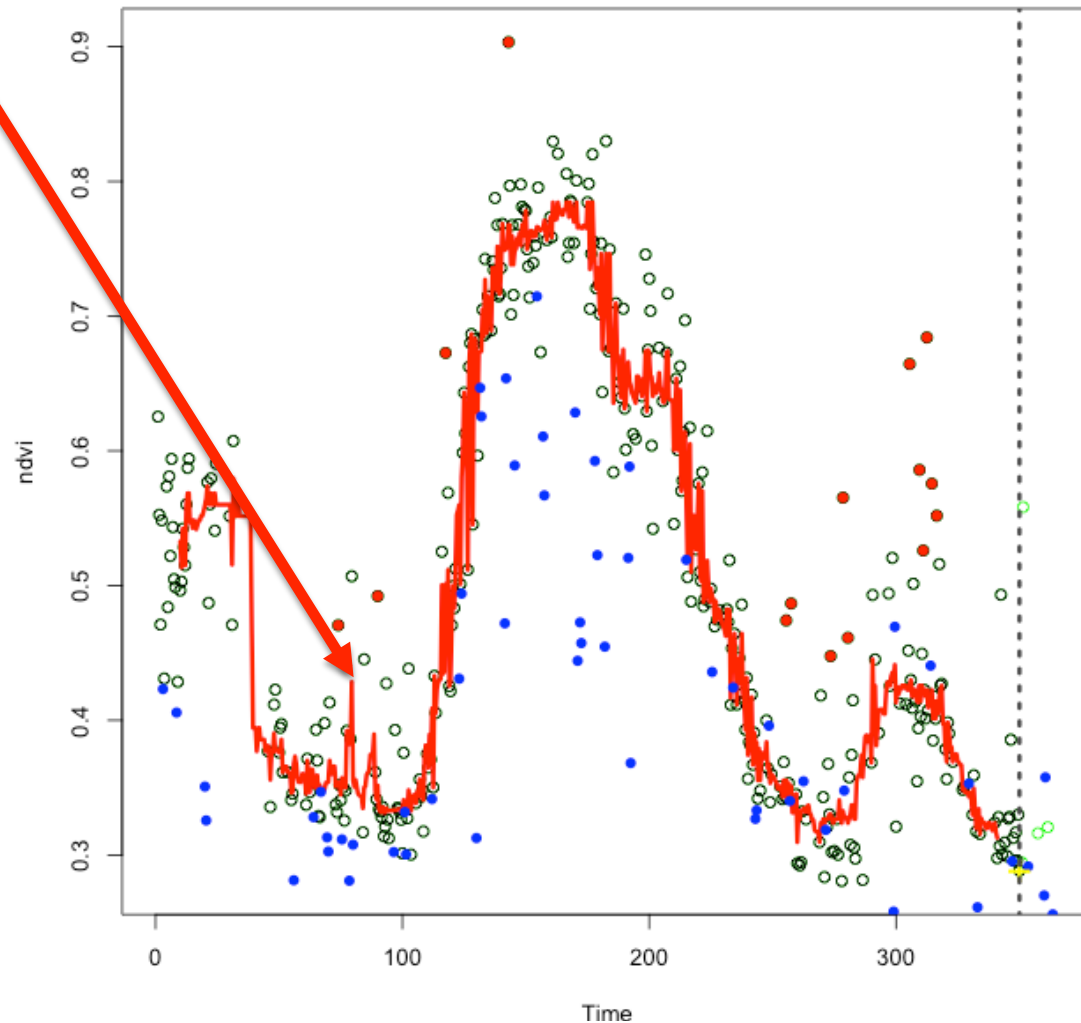
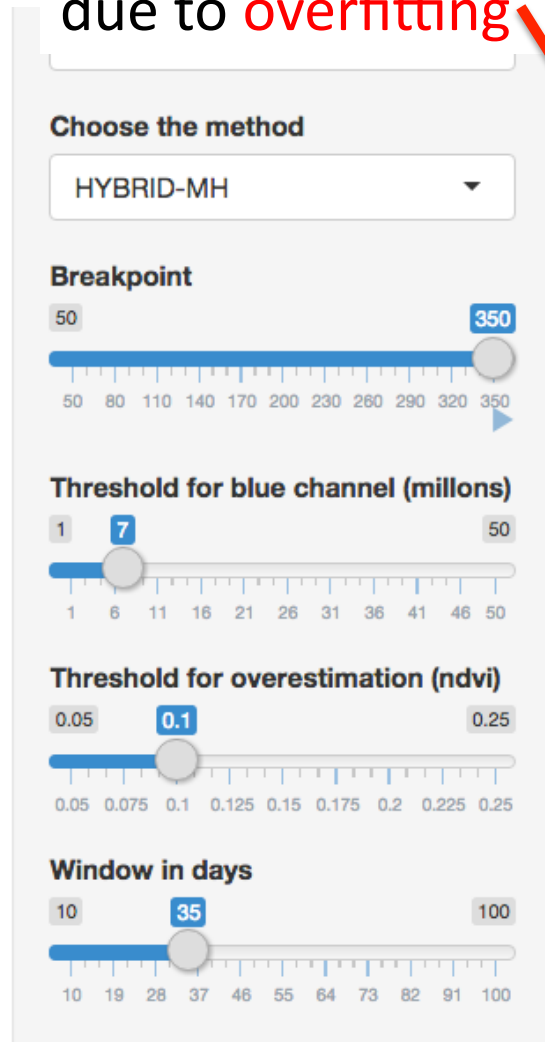
Noise detected by
the **cycle fitting**

Noise detected by
the **blue channel**



How to Automatically Avoid Overfitting ?

False variations
due to **overfitting**



Thanks

References

Ren, Huazhong; Du, Chen; Liu, Rongyuan; Qin, Qiming; Yan, Guangjian; Li, Zhao-Liang; Meng, Jinjie (2014). Noise Evaluation of early images for Landsat 8 Operational Land Imager. OPTICS EXPRESS, 22(22), 27270-27280.

G. Lisini, F. Dell'Acqua, G. Trianni, P. Gamba, "Comparison and combination of multiband classifier for Landsat urban cover mapping", Proc of IGARSS'05, Seoul (Korea), 25-29 July 2005.

Steven P. Brumby, James P. Theiler, Jeffrey J. Bloch, Neal R. Harvey, Simon J. Perkins, John J. Szymanski, and Aaron C. Young. Evolving land cover classification algorithms for multispectral and multitemporal imagery. In Michael R. Descour and Sylvia S. Shen, editors, Imaging Spectrometry VII, volume SPIE-4480, pages 120–129, January 2002. The International Society for Optical Engineering.

Sato, H. P. and Tateishi, R., 2004, Land cover classification in SE Asia using near and short wave infrared bands. International Journal of Remote, 25, 2821–2832 .

Jianjun Qiu, Huajun Tang, Steve Froking, Stephen Boles, Changsheng Li, Xiangming Xiao, Jiyuan Liu, Yahui Zhuang & Xiaoguang Qin (2003). Mapping Single-, Double-, and Triple-crop Agriculture in China at $0.5^\circ \times 0.5^\circ$ by Combining County-scale Census Data with a Remote Sensing-derived Land Cover Map.

Simonetti E., Simonetti D., Preatoni D. (2014). Phenology-based land cover classification using Landsat 8 time series. JRC Technical Reports.